Yavuz *BMC Chemistry* (2024) 18:146
https://doi.org/10.1186/s13065-024-01241-z

BMC Chemistry

RESEARCH

Open Access

Synthesis of new two 1,2-disubstituted benzimidazole compounds: their in vitro anticancer and in silico molecular docking studies

Sevtap Caglar Yavuz[1*]

Abstract
In this study, two new molecules were synthesized from the reaction of 2-methyl-1*H*-benzo[*d*]imidazole with aryl halides in the presence of a strong base. The structures newly of synthesized 1,2-disubstituted benzimidazole compounds were characterized using spectroscopic techniques (FT-IR, ^{1}HNMR, ^{13}CNMR) and chromatographic technique (LC/MS). For discovering an effective anticancer drug, the developed heterocyclic compounds were screened against three different human cancer cell lines (A549, DLD-1, and L929). The results demonstrated that of IC50 values of compound **2a** were higher as compared to cisplatin for the A549 and DLD-1 cell lines. The frontier molecular orbital (FMO), and molecular electrostatic potential map (MEP) analyses were studied by using DFT (density functional theory) calculations at B3LYP/6-31G** level of theory. The molecular docking studies of the synthesized compound with lung cancer protein, PDB ID: 1M17, and colon cancer antigen proteins, PDB ID: 2HQ6 were performed to compare with experimental and theoretical data. Compound **2a** had shown the best binding affinity with -6.6 kcal/mol. It was observed that the theoretical and experimental studies carried out supported each other.

Keywords 1,2-disubstituted benzimidazole, DFT, Spartan 10, Anticancer activity, Cytotoxicity studies, ADMET, Molecular docking

Introduction

Heterocycles are the basis of drug discovery and form the core structure of approximately 80% of pharmaceuticals [1]. The benzimidazole nucleus, a heterocyclic compound with a broad spectrum of biological activity, is considered a biological pharmacophore [2]. There is a wide variety of drugs available that have benzimidazoles as their core, examples of some of the few blockbuster drugs such as candesartan, omeprazole, and albendazole [3]. Benzimidazole derivatives also easily interact with the biopolymers of living systems, being structural isosteres of inherently consisting nucleotides [4], and are widely used in the improving of recent curative agents against many illnesses. Benzimidazole and its derivatives, which have been extensively researched in the pharmaceutical field, have versatile pharmacological properties that are very useful in drug development. Many pharmacological activities have been described for benzimidazole derivatives, anti-cancer, anti-tubercular, anti-acetylcholinesterase, anti-viral, anti-protozoal, analgesic, anti-malarial,

*Correspondence:
Sevtap Caglar Yavuz
sevtap.yavuz@erzincan.edu.tr
[1]Department of Medical Services and Technicians, Ilic Dursun Yildirim Vocational School, Erzincan Binali Yildirim University, Erzincan, Türkiye

anti-inflammatory, anti-fungal, and anti-histamine [5–11]. The different activities of benzimidazole and its derivatives may result from different groups on the benzimidazole nucleus [12].

Cancer is one of the deadliest diseases in the world. This disease, which begins with the abnormal and uncontrolled growth of cells, destroys body tissue and causes metastasis [13, 14].

The death rate from cancer is set to almost double in the coming years, according to an info issued by the World Health Organization (WHO) [15].

Biological therapies such as radiotherapy, chemotherapy, surgery, immunotherapy, hormone therapy, and gene therapy can be used alone or in combination in the treatment of cancer [16]. Due to the complex nature of cancer, there are currently no drugs that can destroy only cancer cells in patients [17]. The majority of methods used to treat many cancer diseases are toxic, and have caused morbidity [18].

Therefore, there is a great need to develop new cancer treatment approaches to target only cancer cells without harming normal cells and to discover new and powerful chemotherapeutics with minimal side effects. Although there are few anticancer drugs containing benzimidazole core (nokodazole, carbendazim, bendamustine) (Fig. 1) on the market, there are many studies in the literature on the anticancer effectiveness of benzimidazoles.

The epidermal growth factor receptor (EGFR) is a family of cellular transmembrane tyrosine kinases that are overexpressed in many human tumors, including colorectal, prostate, ovarian, breast, and lung cancers. Abnormal activation of EGFR is common in many types of cancer and is associated with apoptosis, angiogenesis, and metastasis [19].

Cyclophilins (Cyps) are a family of proteins that are ubiquitous in organisms and have biological functions such as promoting intracellular protein folding and participating in pathological processes such as inflammation and tumors. Cyps inhibit the proliferation and differentiation of cells and support apoptosis. Cyps are also known to be involved in many pathological processes including viral infections, cardiovascular disease, inflammatory responses, and cancer [20].

Focal adhesion kinase (FAK) is a non-receptor tyrosine kinase. FAK is involved in tumor growth and various cell functions, including motility, proliferation, adhesion, metastasis, apoptosis, chemo-resistance, and angiogenesis, related to integrin signal transduction. In many cancers, such as prostate, lung, and breast cancer, FAK expression has been detected. Therefore, FAK is expected to serve as a new potential target in tumor therapy [21].

The phosphatidylinositol 3-kinase (PI3K)/AKT/mammalian target of rapamycin (mTOR) signalling pathway is the significant intracellular pathways regulating cell growth, motility, metabolism and angiogenesis. Activating the PI3K/AKT/mTOR pathway helps improving of tumor and endurance to cancer treatments. In almost all human cancers, such as breast cancer, colorectal cancer, and haematological malignancies, the PI3K/AKT/mTOR signalling pathway has been reported to be dysregulated. The efficacy of PI3K inhibitors in inhibiting tumor progression is becoming increasingly clear [22].

Due to the information provided above, EGFR, Cyps, FAK, and PI3K proteins for molecular docking were used as a target.

In-silico drug design or computer-aided drug design is made predictable by computer simulations and modeling of many important parameters related to molecules that can be drug candidates, using different sub-fields of artificial intelligence. It is generally use high performance molecular dynamics simulation software (GROMACS, AMBER, and NAMD etc.) [23–27] known for their extensive simulation capabilities and accuracy, and molecular docking software (SeeSAR and Autodock etc.) [23, 28].

Benzimidazole is a heterocyclic ring that is frequently used in drug development due to its different biological and pharmacological effects and is an important structure that plays a key role in new drug candidates. In this study, two 1,2-disubstituted benzimidazole compounds were designed and synthesized that may have new potential anticancer effects. The docking analysis were carried

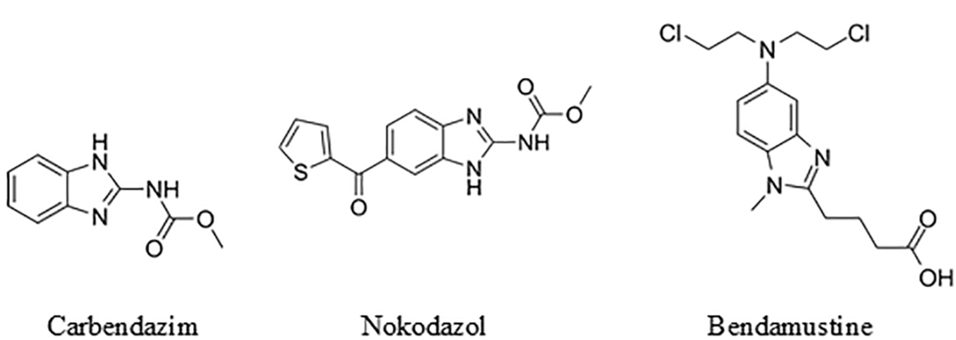

Fig. 1 Chemical structure of some commercial benzimidazole-derived anticancer drugs

out using UCSF Chimera software with its AutoDock Vina tool. The cytotoxic effects of the compounds **2a** and **2b** on A549, DLD-1, and L929 cell lines were tested for 48 h.

With respect to the outcomes acquired compound **(2a)** had cytotoxic activities against human cancer cell lines (A549, DLD-1, and L929) with IC50 values of 111.70, 185.30, and 167.3 mM, respectively. The potential mechanism of action for these two compounds was explored through molecular docking. In addition, DFT computations were achieved using the B3LYP/6-31G** basis set to predict the structural and electronic features of the synthesized novel benzimidazole derivatives. Thanks to the FMO analysis of the compounds, an idea was obtained about their chemical reactivity and stability. MEP maps of the compounds were obtained in three dimensions and regions open to electrophilic and nucleophilic attacks were identified.

Materials and methods

Chemicals & equipments

The essential chemical substances, such as 2-methylbenzimidazole, 3-chlorobenzyl chloride, 2,3,5,6-tetramethylbenzyl chloride, ethyl alcohol (EtOH), potassium hydroxide (KOH) were purchased from Sigma-Aldrich, Merck, and Isolab. ^{1}HNMR (400 MHz) spectra and ^{13}CNMR (100 MHz) spectra were recorded on a Bruker AM 400 MHz NMR spectrometer with DMSO-d6 as the solvent. The FT-IR analysis was performed by FT-IR spectrometer (Nicolet 6700, Thermo Scientific). LC-MS/MS spectra were recorded using a Shimadzu 8040 LC-MS spectrophotometer. The compounds were prepared according to the literature [29, 30] (Scheme 1). KOH is a prototypical strong base used in a variety of laboratory and chemical synthesis applications due to its effectiveness and reliability in providing high concentrations of hydroxide ions. In this study, we used KOH, which is a strong base. The reaction was conducted at 80 °C for 12 h.

Synthesis procedure of compound 2a

2-methylbenzimidazole (0.5 g) was dissolved in EtOH (4 ml), and KOH (0.004 mol) was added to this solution. It was mixed 1 h at 25°C. Then, 3-chlorobenzyl chloride (0.003 mol) was slowly added to this solution, and the reaction mixture was stirred for 12 h at 80 °C. The aimed final product was washed a few times with EtOH and dried under vacuum.

Color: Cream. IR: 1447 (C=N); 2916 and 3043 cm^{-1} (C-H). ^{1}HNMR (400 MHz, DMSO-d$_6$, 298 K), δ: 2.51 (s, 3*H*, $CH_2NCC\mathit{H}_3$); 5.49 [s, 2*H*, $NC\mathit{H}_2C_6H_4$(Cl)-3]; 7.02–7.57 (m, 8*H*, Ar-*H*). ^{13}CNMR (100 MHz, DMSO-d$_6$, 298 K), δ: 13.8 ($CH_2NC\mathit{C}H_3$); 46.1 [$N\mathit{C}H_2C_6H_4$(Cl)-3]; 152.6, 142.0, 139.6, 135.3, 133.9, 131.2, 128.1, 126.8, 125.7, 122.6, 118.6, 114.6, 110.5 (Ar-*C* and N*C*N). Elemental analysis for $C_{15}H_{13}N_2Cl$ (256.74 g/mol) %: Found C: 70.05; H: 5.21; N: 10.82. Anal. Calc. C: 70.17; H: 5.10; N: 10.91. LC/MS (*m/z*): Anal. Calcd. for $C_{15}H_{13}N_2Cl$ is 256.74; found is 257.

Synthesis procedure of compound 2b

2-methylbenzimidazole (0.5 g) was dissolved in EtOH (4 ml), and KOH (0.004 mol) was added to this solution. It was mixed 1 h at 25 °C. Then, 2,3,5,6-tetramethylbenzyl chloride (0.003 mol) was slowly added to this solution, and the reaction mixture became cloudy after a while. The reaction mixture was stirred for 12 h at 80 °C. The aimed final product was washed a few times with EtOH and dried under vacuum.

Color: White. IR: 1436 (C=N); 2918 and 3054 cm^{-1} (C-H). ^{1}HNMR (400 MHz, DMSO-d$_6$, 298 K), δ: 2.05, 2.19, and 2.37 [s, 15*H*, $CH_2NCC\mathit{H}_3$ and $NCH_2C_6H(C\mathit{H}_3)_4$]; 5.42 (s, 2*H*, $NC\mathit{H}_2C_6H_4(CH_3)_4$); 6.76–7.49 (m, 5*H*, Ar-*H*). ^{13}CNMR (100 MHz, DMSO-d$_6$, 298 K), δ:14.6, 15.8, and 20.6 [$CH_2NC\mathit{C}H_3$ and $NCH_2C_6H(\mathit{C}H_3)_4$]; 44.5 [$N\mathit{C}H_2C_6H(CH_3)_4$]; 152.8, 142.2, 135.6, 134.0, 132.1, 131.8, 121.9, 121.5, 118.6, 110.6 (Ar-*C* and N*C*N). Elemental analysis for $C_{19}H_{22}N_2$ (278.40 g/mol) %: Found C: 82.08; H: 7.84; N: 10.04. Anal. Calc. C: 81.97; H: 7.97; N: 10.06. LC/MS (*m/z*): Anal. Calcd. for $C_{19}H_{22}N_2$ is 278.40; found is 279 (See supplementary file for NMR, IR and LC/MS spectra of compounds).

Cytotoxic activity studies

Cytotoxic activity analyses of **2a** and **2b** were carried out by the process designated in the literature [31–34].

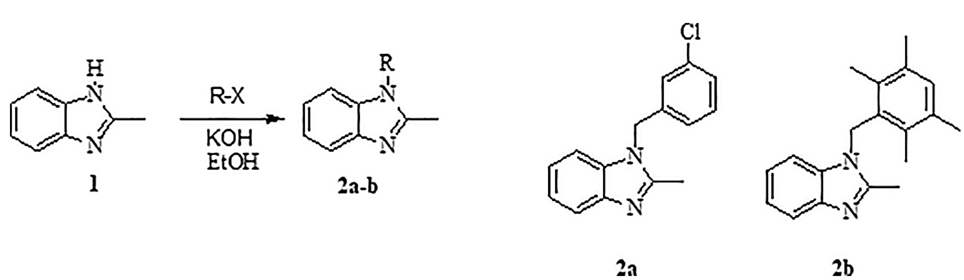

Scheme 1 Reaction representation of 2-methyl-1*H*-benzo[*d*]imidazole with aryl halides

Colon (DLD-1; ATCC® CCL-221™), lung (A549; ATCC® CCL-185™) cancer, cell lines were purchased from the American Type Culture Collection (ATCC, USA). DLD-1, A549, and L929 cells were cultured in Dulbecco's modified Eagle's Medium-high-glucose (DMEM) supplemented with 10% fetal bovine serum (FBS) and 1% GlutaMAX™. After the cells reached 90% density, they were removed from the flask using trypsin-EDTA and counted. The cell seeding was done at a density of 5×10^3 cells/well into sterile 96-well plates. After seeding, the plates were incubated for 24 h. After the incubation period was completed, the medium in the wells was removed and fresh medium was added instead. The DLD-1, A549, and L929 cells were exposed to the compounds **(2a** and **2b)** at 300, 150, 75, 37.5 and 18.75 µM concentrations for 48 h. After the cells were incubated for 48 h, the medium was removed. The MTT stock solution (50 µL, 5 mg/mL) was added to the plate wells and incubated for an additional 2 h. After the 2-hour incubation period, the dye in the medium was carefully slowly removed and 200 µL DMSO was added in its place. It was left to mix slowly for half an hour. Absorbance values were measured in the Epoch 2 Elisa plate reader device at 590 nm. IC_{50} values were calculated by GraphPad Prism Software 5.

Methods of calculation

The theoretical calculations of synthesized compounds were performed using Spartan'10 software packages [35]. The geometry of the synthesized compounds has been optimized by B3LYP method with 6-31G** [36] origin using DFT technique. The docking analyses were accomplished using UCSF Chimera software with its AutoDock Vina tool [37]. Some druggability, pharmacokinetics, and toxicity analyses were estimated owing to online web tools. The used web servers were ADMETlab [38], admetSAR [39], SwissADME [40], Pro Tox-II (Banerjee and Ulker, 2022). Biovia Discovery Studio was used to visualize and analyze the docking results. [41]. Crystal data of the 1M17, 1MP8, 2HQ6, and 1E8X macromolecules are obtained from the RCSB Protein Data Bank website (https://www.rcsb.org/).

Results and discussion

Spectral characterization of compounds 2a and 2b

Two new 1,2-disubstituted benzimidazole compounds were synthesized in one step (Scheme 1). The obtained compounds were characterized by means of FT-IR spectroscopy, ^{1}HNMR, ^{13}CNMR, and elemental analysis. The ^{1}HNMR spectra of the compounds were run at 400 MHz in DMSO-d6, and also ^{13}CNMR spectra of the compounds were run at 100 MHz in DMSO-d6. In ^{1}HNMR, the signal related to a methyl group 2-position on benzimidazole ring resonated upfield at δ 2.51, and 2.39 ppm as 3 H singlets for **2a** and **2b**, respectively. The ^{13}CNMR spectra were run in DMSO-d6 at 100 MHz. The imidazole-linked methyl carbon signals resonated at δ 13.76 ppm for **2a**, δ 14.59 ppm for **2b**. The aryl-linked methyl carbon signals resonated at δ 46.06 ppm for **2a**, and at δ 21.45 ppm and 58.47 ppm for **2b**. The IR spectrum output of the compounds demonstrated the stretching frequencies of the characteristic C=N peak at 1447.81, and 1436.87 cm-1 for **2a** and **2b**, respectively. The stretching frequency bands of C–H were observed at 2916.93 and 3043.48 cm^{-1} for **2a**, 2918.58 and 3054.74 cm^{-1} for **2b**.

Table 1 IC_{50} outcomes for compounds **2a** and **2b** in A549, DLD-1, and L929 cell lines

Compounds	IC_{50} (µM)		
	A549	DLD-1	L929
2a	111.70 ± 6.22	185.30 ± 5.87	167.30 ± 4.79
2b	176.80 ± 4.66	> 300	> 300
Cisplatin	9.79 ± 0.91	55.58 ± 4.05	7.41 ± 0.47

Cytotoxic activity studies

The newly synthesized compounds **2a** and **2b** were tested against three different cell lines as in vitro. Using the MTT assay method, the compounds were appraised for their cytotoxicity at 18.75, 37.5, 75, 150, and 300 µM in the A549, DLD-1, and L929 cell lines. In the study, a positive control drug (cisplatin) was used as a reference compound for comparison under the same experimental conditions. The cancer cell lines were exposed to synthesized compounds for a period of 48 h. The results are given in Table 1.

It is known that colon cancer is a common type of cancer worldwide and can cause death if not diagnosed early. Lung cancer, which occurs as a result of the uncontrolled growth of abnormal cells, is another type of cancer that is most common and causes the most deaths worldwide. For this reason, many studies on lung and colon cancer cell lines continue to be conducted in the literature to find new drug candidates [42, 43]. For this reason, colon and lung cell lines were preferred as cancer cell lines in this study. Mouse fibroblast cell line was used as the healthy cell.

Compound **2a** had cytotoxic effects with IC_{50} values of 111.70±6.22, 185.30±5.87, and 167.30±4.79 µM for A549, DLD-1, and L929, respectively. Compound **2b** had cytotoxic effects with IC_{50} values of 176.80±4.66, >300, and >300 µM for A549, DLD-1, and L929, respectively. Although compound **2b** was found to be inactive in DLD-1 and L929 cell lines, the same compound was found quite less active against A549 cell line. The specifically compound **2a** inhibited the proliferation of A549 cancerous cells rather than DLD-1 cancer cells. Compounds **2a** and **2b** appeared to be much less effective against the A549 and DLD-1 cell lines than the reference drug.

While compound **2a** has the chloro group on the benzyl ring at the 3-position, compound **2b** contains substituents with the methyl group at the 2,3,5,6-positions. Compound **2a** showed better, albeit low, activity against the cell lines studied than compound **2b**.

The different substituents on the benzyl ring (electron donating or withdrawing) may be responsible for these differences.

The change in viability rates depending on concentration is given in Figs. 2, 3 and 4. Compound **2b** was the medicine candidate with the least efficient level. Even when used at a high concentration of 300 µM, a cell viability rate of around 40% was observed. Therefore, compound **2b** does not have a high toxic effect on A549, DLD-1, and L929 cell lines.

Compound **2a**, which has a chloride group, was the more potent compound than compound **2b** and induced significant cytotoxicity at 150 and 300 µM. Compound **2a** showed cytotoxicity, especially at a concentration of 300 µM. The compound 2-methyl-3-(3-chlorobenzyl)benzimidazole **2a** can inhibit DNA replication and transcription by binding or intercalating with DNA. This effect can stop cell division and lead to apoptosis in cancer cells.

The compounds (**2a**, **2b**) inhibited the proliferation of fast cell division lung cancerous cells rather than colon and fibrosarcoma cancerous cells. Inactive compound 2b appears to be able to inhibit the growth of colon cells only at the highest concentration 300 µM. It was found that compound 2a inhibited the growth of colon cells more at 300 and 150 µM.

Computational studies

The FMOs are called the highest occupied molecular orbital (HOMO) and the lowest unoccupied molecular orbital (LUMO). [44]. According to Fukui's FMO theory, the chemical reactivity of the molecule in terms of HOMO or LUMO electron density is interpreted and helps us know how electric charges move within the molecule. While the HOMO molecular orbital symbolizes the highest occupied orbital filled by electrons, the LUMO orbital is described as the lowest unfilled orbital

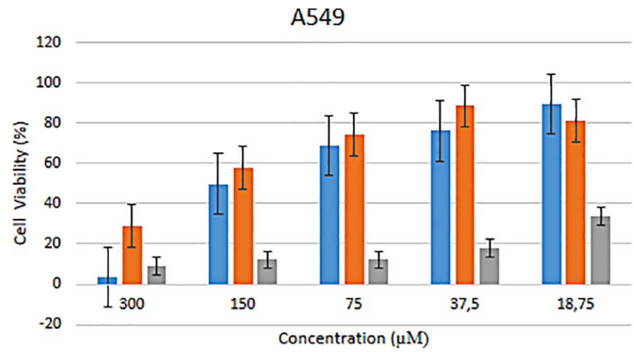

Fig. 2 Cell viability ratio of A549

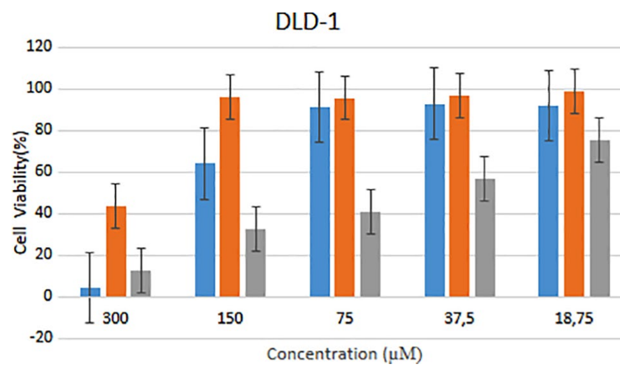

Fig. 3 Cell viability ratio of DLD-1

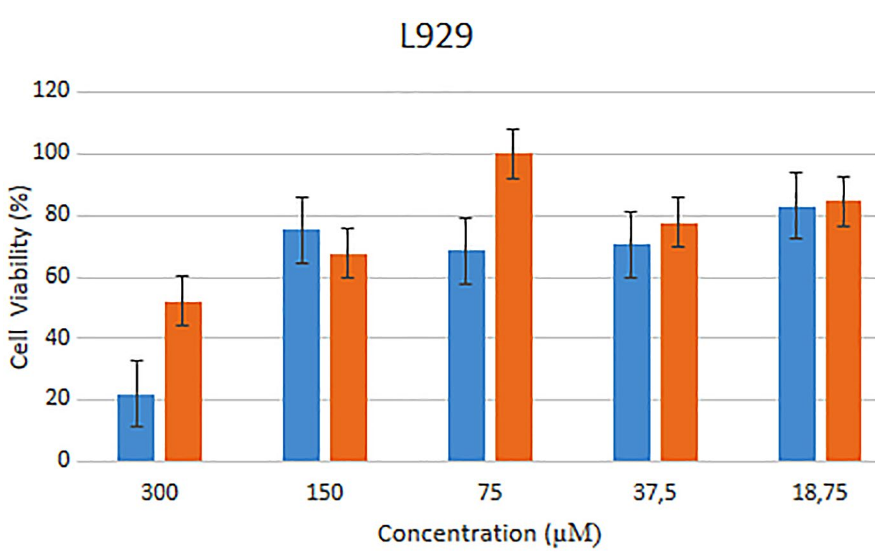

Fig. 4 Cell viability ratio of L929 (Noted: blue: **2a**, orange: **2b**, and gray: cisplatin)

Table 2 Effect of solvents on the HOMO-LUMO energies for compounds **2a** and **2b**

Medium	Compound	$E_{HOMO(eV)}$	$E_{LUMO(eV)}$	$\Delta E_{(eV)}$
gas	*(2a)*	-5.9043	-0.6482	5.2561
water		-6.1917	-0.5252	5.6665
ethanol		-6.1877	-0.5271	5,6606
gas	*(2b)*	-5.6877	-0.1896	5.4981
water		-6.1075	-0.4631	5.6444
ethanol		-6.0908	-0.4476	5.6432

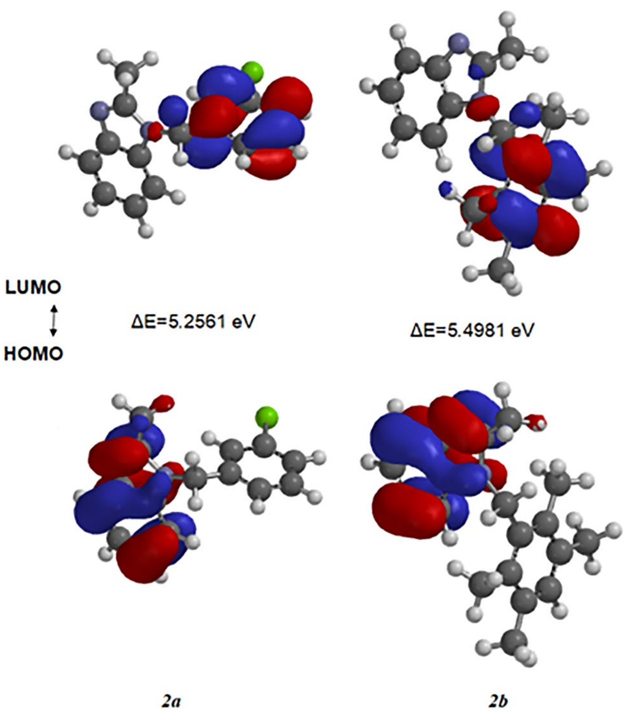

Fig. 5 HOMO and LUMO orbitals for compounds **2a** and **2b**

[45]. FMOs are significant parameters in quantum chemistry that play a role in defining the global and local properties of the molecule. The larger the gap between HOMO-LUMO orbitals, the harder and the less reactive the molecule will be as electron flow will be less. On the other hand, the smaller the HOMO-LUMO gap, the softer the molecule and the more reactive it is. Parameters such as molecular chemical hardness, electronegativity, chemical potential, and softness were calculated using HOMO and LUMO energies. Effect of different solvent mediums on the HOMO-LUMO energies for compounds **2a** and **2b** were shown in Table 2, it is possible to see that the water environment had the highest energy range with a value of 5.6665 eV and 5.6444 eV, respectively. For the title compounds, especially in the aqueous environment, the ΔE energy gaps were larger than in the gaseous environment and methanol environment. HOMO and LUMO orbitals for title compounds were displayed in Fig. 5. For compound **2a**, E_{HOMO}=-5.9043 eV, E_{LUMO}=-0.6482 eV, and ΔE=5.2561 eV were found. The fact that the structure has high energy range, high hardness (η=2.6281 eV), and low softness parameters (σ=0.1902 eV) shows that it is quite stable with low chemical activity and high kinetic stability. For compound **2b**, E_{HOMO}=-5.6877 eV, E_{LUMO}=-0.1896 eV, and ΔE=5.4981 eV were found. Its high hardness (η=2.7491 eV) and low softness parameter (σ=0.1819 eV) indicate that this compound has high chemical stability and low reactivity. The chemical potential values of compounds **2a** and **2b** were determined to be -3.2763 eV and −2.9387 eV, respectively and the electronegativity index values were 3.2763 eV and 2.9387 eV, respectively. In gaseous environment the calculated energy gap values are less than 5 eV, which stands for that this compounds are a good bioactive material. Other chemical reactivity parameters of the synthesized compounds were shown in Table 3.

Table 3 Global reactivity descriptors of the title molecules in the gaseous ambient

	(2a)	(2b)
Parameters	Values(eV)	
E_{HOMO}	-5.9043	-5.6877
E_{LUMO}	-0.6482	-0.1896
Energy band gap ($\Delta E = E_{LUMO}-E_{HOMO}$)	5.2561	5.4981
Ionization potential ($I = -E_{HOMO}$)	5.9043	5.6877
Electron affinity ($A = -E_{LUMO}$)	0.6482	0.1896
Electronegativity ($\chi =(I + A)/2$)	3.2763	2,9387
Chemical hardness ($\eta= (I-A)/2$)	2.6281	2.7491
Chemical softness ($\sigma = 1/2\eta$)	0.1902	0.1819
Chemical potential ($\mu = -(I + A)/2$)	-3.2763	-2,9387
Electrophilicity index ($\omega = \mu^2/2\eta$)	2.0422	1.5707
Maximum charge transfer index ($\Delta N_{max} = -\mu/\eta$)	1.2466	1.0689

In order to understand the charge distribution of the synthesized compounds, the results obtained from the calculations made with the B3LYP/6-31G** level were visualized in three dimensions using the Spartan'10 program. Obtained resulting molecular electrostatic potential surface maps are given in Fig. 6.

Dissimilar values of the electrostatic potential on the surface are given in distinct colors (blue to red). In MEP maps, the red regions show nucleophilic regions, which are atoms or groups of atoms rich in electron density, while the blue regions show electrophilic regions, which are atoms or groups of atoms that are poor in electron density. The green color points out neutral electrostatic potential [46]. In Fig. 6, both mono-chloro and tetramethyl substituted benzene have a high electron density inside the aromatic ring (red color). This means that the aromatic C-H has become more basic.

Molecular docking

Molecular docking computations are an important calculation technique that estimates the binding affinity of ligands to receptor proteins in molecular pharmaceuticals

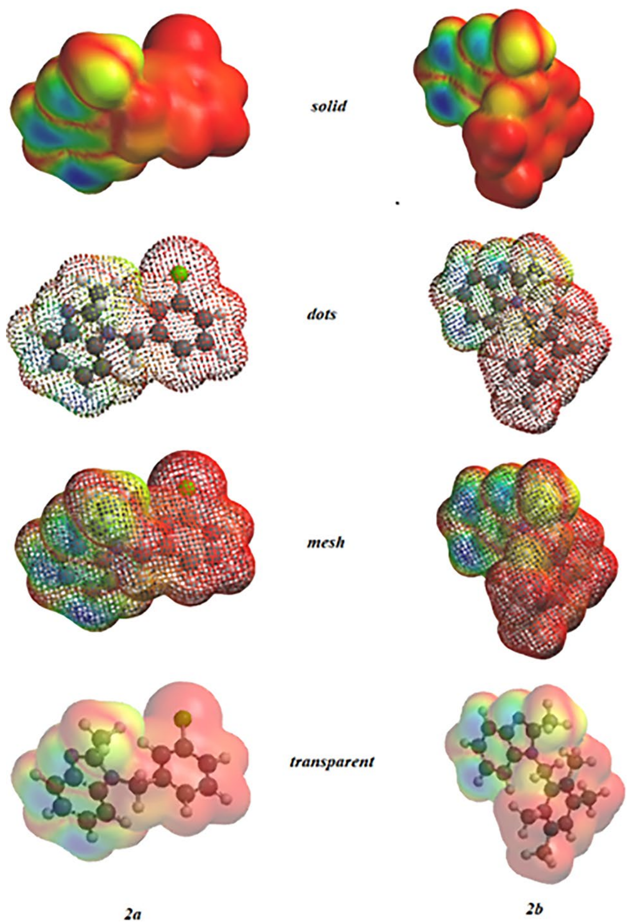

Fig. 6 MEP surfaces of compounds **2a** and **2b**

[47]. Benzimidazole derivatives are compounds that can contribute to designing efficient bioactive molecules for the discovery and development of innovative drugs, particularly in the therapy of cancer [48]. Benzimidazole derivatives have been often used for their anticancer activity against different human cancer cell lines [49, 50]. Therefore, it was performed molecular docking of the compound **2a** with anticancer protein targets from colon cancer (PDB code: 2HQ6), tumor invasion and metastasis (PDB code: 1MP8), cancer cells proliferation and tumor growth (PDB code: 1E8X) and lung cancer (PDB code: 1M17). Active sites of proteins were described as including residues at the centre of the active site of the protein. A grid box size of 30 Å × 30 Å × 30 Å was used for the grid generation in all docking studies. The molecules were optimized using the Spartan'10 package program for molecular docking calculation. It was created .pdb file of optimized structure. In the computations performed using these files, the biological activities of molecule **2a** were compared with the proteins known in the stages of colon cancer and lung cancer. Good energy values of the docking results (-6.6 kcal/mol, -6.4 kcal/mol, -4.8 kcal/mol, and −3.9 kcal/mol respectively) for PDB ID: 1M17, PDB ID: 1MP8, PDB ID: 2HQ6 and PDB ID: 1E8X of molecule **2a** were shown in Table 4. Molecule **2a** constituted secondary interactions (van der Waals, hydrogen bonding, π-anion, π-sigma, alkyl, and π-alkyl) with the EGFR tyrosine kinase (1M17). On the other hand same molecule constituted secondary interactions (van der Waals, π-cation, amide-π stacked, alkyl, and π-alkyl) with the 2HQ6 protein which identified serologically as the cyclophilin CeCYP16-like domain of colon cancer. Hydrogen bonds describe principle stabilization potencys in biomolecular structure. Van der Waals forces are also very important in the formation of protein-ligand complexes, and it is noted that these interactions are important in determining the binding affinity of the ligand to the protein. On the other hand, the hydrophobic interaction types such as π alkyl, π-sigma, and π-π stacked, types of electrostatic interactions as attractive charge, pi-anion, pi-cation interactions assist increase the interaction of the ligand in the binding pocket of the receptor [51]. It can be seen in Figs. 8 and 10 that 1MP8 and 1E8X proteins also make secondary interactions with compound **2a**. Such bonds encountered in docking analyses are important for the structural unity of many biological molecules such as protein and DNA, as well as for drug-receptor interactions. These interactions are shown in Figs. 7, 8, 9 and 10.

In silico pharmacokinetics/ADME-Tox studies

Computer-aided approaches are able to potential to accelerate drug discovery in terms of help minimize the costs, and reduce the time [52]. Computer-aided drug discovery includes in silico assessment, modification, analysis and optimization of computational identification of potential drug targets [53]. According to Lipinski rule, the molecule should comply specific factors to be improved as an orally drug [54]. According to Lipinski rule, these parameters are: molecular weight (should be ≤500 Dalton), hydrogen bond acceptor (should be number of HBAs ≤ 10), hydrogen bond donor (should be number of HBDs ≤ 5), lipophilicity (should be clogP < 5) and number of rotatable bonds (should be < 10) [55]. The pharmacokinetics/ADME results demonstrated that synthesized compounds comply with Lipinski rule. These compounds displayed molecular weight less than 500 proposing that these compounds can be well moved in the body. In 80% of the total drugs the molecular weight is below 450 daltons. When a compound meets these rules, it is more likely to have cell membrane permeability and be easily absorbed in the body [56, 57]. To be an effective medicine, a substance must be soluble in both water and oil. Medicines taken by mouth must pass through the intestinal lining and penetrate the cell membrane to reach the interior of a cell. The model compound for the cell membrane is octanol, known as log

Molecular structure	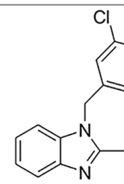 **2a**		
PDB ID	**Docking Score (kcal/mol)**	**RMSD**	**Amino Acid Residues**
1M17	-6.6	1.793	LEU23, VAL31, ALA48, LYS50, LEU97, LEU149, ASP160
1MP8	-6.4	1.984	ILE15, VAL23, ALA37, LYS39, CYS87, LEU138
2HQ6	-4.8	2.019	ARG54, ALA100, ASN101, ALA102, LEU121, LYS124, HIS125
1E8X	-3.9	2.051	LEU671, SER672, TRP674, LYS676, LYS678, CYS679, PHE685, ALA688

Table 4 Molecular docking results of the molecule **2a**

Pow and this value stands for the octanol/water partition coefficient. Low lipophilicity (logP<5) frequently contributes to good oral absorption land high solubility. Another importance of this coefficient is that it is used as a descriptive in the calculations made for the blood-brain barrier (BBB) in an aqueous environment. One of

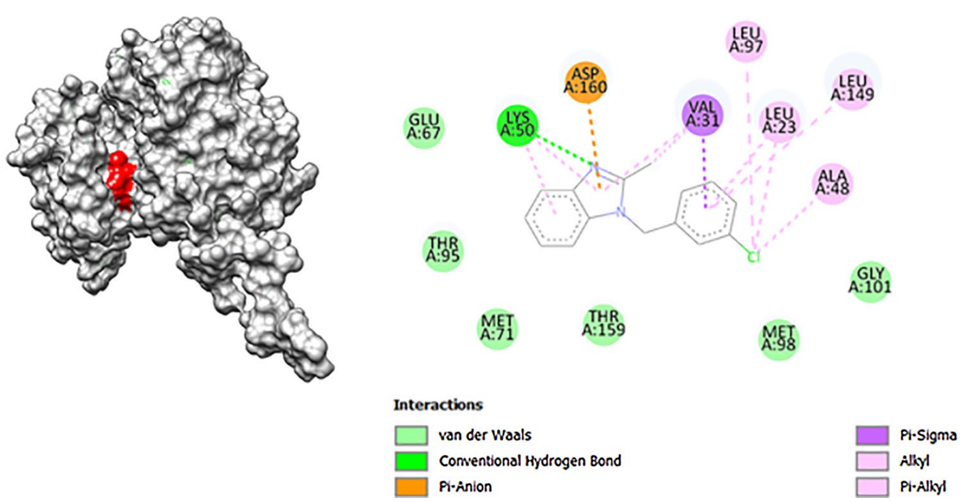

Fig. 7 Graphs of the protein-ligand interaction for the most steady complexes (PDB ID: 1M17)

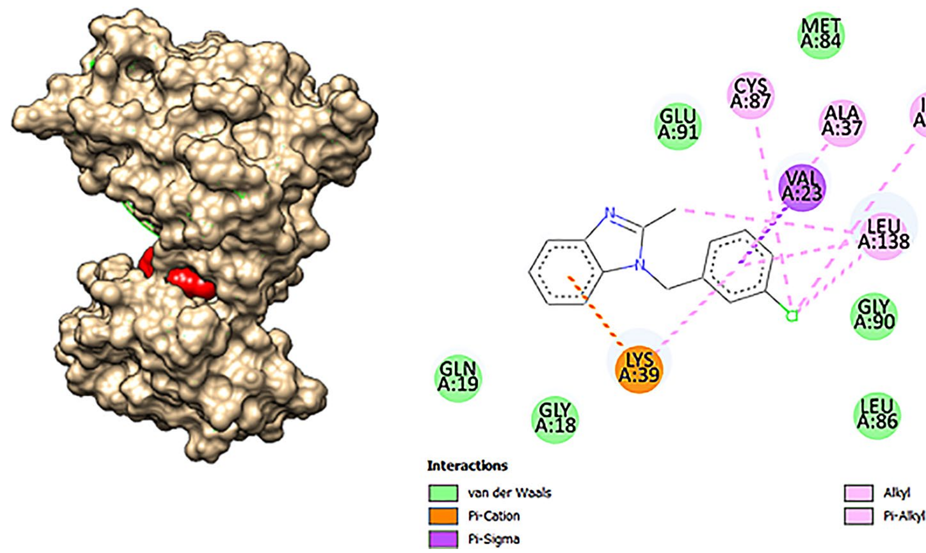

Fig. 8 Graphs of the protein-ligand interaction for the most steady complexes (PDB ID: 1MP8)

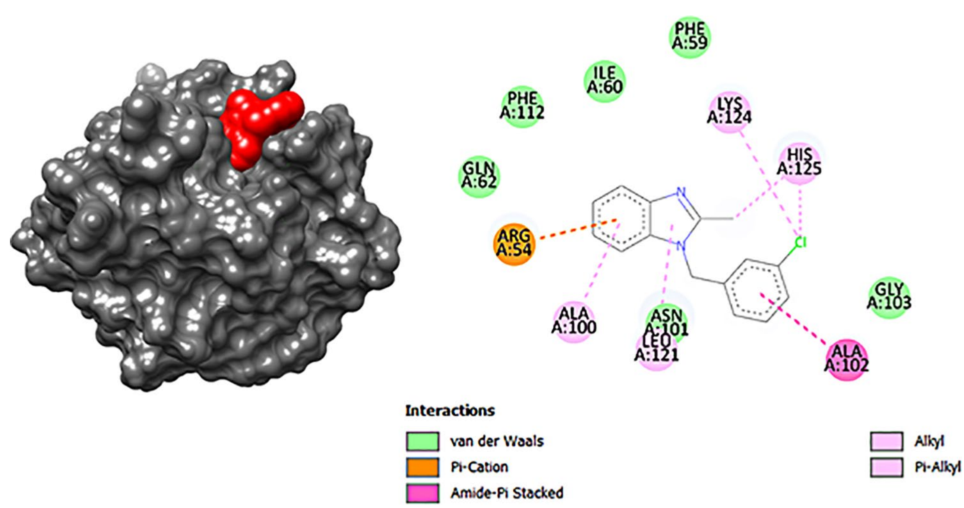

Fig. 9 Graphs of the protein-ligand interaction for the most steady complexes (PDB ID: 2HQ6)

Table 5 Physicochemical properties predictions of the synthesized compounds **2a** and **2b**

Comp. No.	Lipinski parameters									
	MW[a]	HBA[b]	HBD[c]	iLogP[d]	Molar Ref.[e]	Violations	nROTB[f]	TPSA[g]	BBB[h]	GI ABS[i]
2a	256.73	1	0	2.62	75.46	0	2	17.82	Yes	High
2b	278.39	1	0	3.08	90.31	0	2	17.82	Yes	High

[a] Molecular weight. [b] Hydrogen Bond Acceptor. [c] Hydrogen Bond Donor. [d] Partition Coefficient. [e] Molar Refractivity. [f] Number of rotable bonds. [g] Topological Polar Surface Area. [h] Blood Brain Barrier. [i] Gastrointestinal absorption.

the most important features for drug candidate molecules is the ability to cross the BBB. It is especially essential for drugs used in central nervous system diseases to pass through the BBB. It was predicted exhibit high gastrointestinal (GI) absorption and BBB permeability of the synthesized compounds. It cannot be concluded that the compounds have exactly the desired pharmacokinetics required for the development of an orally available drug.

Drug likeness evaluation for the compounds (**2a**, **2b**) is assessed on their in silico pharmacokinetics studies depended on the Lipinski rule (Table 5).

Toxicity analysis was carried out using the Protox-II online tool [58] which ensures knowledge about carcinogenicity, immunotoxicity, mutagenicity, and cytotoxicity related to the compounds. It has acute toxicity estimation findings such as toxicity class classification from 1 (toxic) to 6 (non-toxic). It was estimated that the synthesized

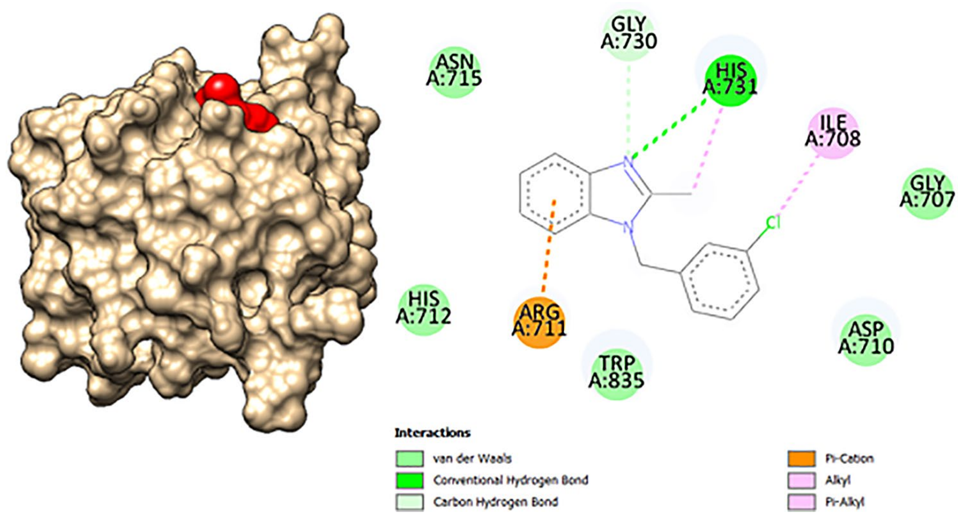

Fig. 10 Graphs of the protein-ligand interaction for the most steady complexes (PDB ID: 1E8X)

Table 6 The toxicity computation of synthesized **2a** and **2b** by Pro-tox II web tool

	Tox. class	Organ toxicity (probability)				
Comp.		Hepatotoxicity	Carcinogenicity	Immunotoxicity	Mutagenicity	Cytotoxicity
2a	IV	Inactive	Inactive	Inactive	Inactive	Inactive
2b	IV	Inactive	Inactive	Inactive	Active	Inactive

compounds were classified as acute toxicity class 4 (slightly toxic). The results recommend that compound **2a** is non-carcinogenic and has no effect on immunotoxicity, cytotoxicity, and mutagenicity. On the other hand, it shows that the **2b** compound is active on mutagenicity (Table 6).

Conclusion

Two 1,2-disubstituted benzimidazole compounds were synthesized, characterized, offered, and debated herein. DFT analysis of the molecular structure, together with the HOMO-LUMO orbitals, was carried out by using the Spartan'10 program software. Assessment of the anticancer activity of new compounds was performed and demonstrated moderate activity also the compounds showed good inhibitory activity against molecular docking. The pharmacokinetic properties of the synthesized molecules were predicted using ADMET, and **2a** molecule has no toxic effect were kept as hepatotoxicity, carcinogenicity, immunotoxicity, mutagenicity, and cytotoxicity. However, molecule **2b** has only mutagenicity toxicity. The ProTox-II program used to predict various toxicological properties of compounds is not sufficient on its own and has classified synthesized compounds as acute toxicity class 4 (slightly toxic). In vitro studies also support this prediction. In particular, compound **2b** was found to be toxic to two human cell lines (DLD-1 and L929).

In this study, the synthesized compounds **2a** and **2b** were tested in vitro against different cancer cell lines. The results showed that **2a**, had slightly antiproliferative activity compared to cisplatin for the A549, DLD-1, and L929 cell lines while **2b** was only found to be active against A549 cell line. The molecular docking behaviour of compound **2a** with lung cancer protein, PDB ID: 1M17 and colon cancer antigen proteins, PDB ID: 2HQ6 and PDB ID: 1E8X were compared with experimental and theoretically. The predicted binding energies were found to be -6.6 kcal/mol, -4.8 kcal/mol, and -3.9 kcal/mol respectively. The docking results showed that compound **2a** was inhibited through secondary interactions. Compound **2a** compared to compound **2b** was softer and more reactive because the HOMO-LUMO energy gap is smaller than compound **2b**. It could be said that compound **2a** showed better biological activity than compound **2b** in the in vitro analyses. It showed that substituents with electron withdrawing capacity (-Cl), as in compound **2a**, make the molecule polar and show good activity. In general, it could be said that compound **2a** may exhibit a therapeutic potential for the prevention of lung cancer based on the cytotoxic analyses obtained. It can be concluded that these compounds affect the inhibitory potential depending on whether the substituents have electron-withdrawing or electron-donating properties.

Supplementary Information

The online version contains supplementary material available at https://doi.org/10.1186/s13065-024-01241-z.

Supplementary Material 1

Acknowledgements
The author thank Erzincan Binali Yildirim University-Scientific Research Unit for supplying under grant project number FBA-2023-865 and go to Senem Akkoc for giving support for the cytotoxicity studies.

Author contributions
S.C.Y: Conceptualization, Methodology, Visualization, Investigation, Writing original draft, review, and editing.

Funding
Erzincan Binali Yildirim University-Scientific Research Unit: FBA-2023-865.

Data availability
All data generated or analyzed during this study are included in this published article and its Supplementary information files. Analytical data including copies of mass spectra, FT-IR, ^{1}HNMR, and ^{13}CNMR is available in the Supplementary information.

Declarations

Ethics approval and consent to participate
Not applicable.

Consent for publication
Not applicable.

Competing interests
The authors declare no competing interests.

Received: 4 April 2024 / Accepted: 4 July 2024
Published online: 07 August 2024

References

1. Mahurkar ND, Gawhale ND, Lokhande MN, Uke SJ, Kodape MM, Benzimidazole. A versatile scaffold for drug discovery and beyond-a comprehensive review of synthetic approaches and recent advancements in medicinal chemistry. Results Chem. 2023;6:101139. https://doi.org/10.1016/j.rechem.2023.101139.
2. Narasimhan B, Sharma D, Kumar P. Benzimidazole: a medicinally important heterocyclic moiety. Med Chem Res. 2012;21:269–83. https://doi.org/10.1007/s00044-010-9533-9.
3. Saha P, Kour P, Kumar R, Sharma DK. $K_2S_2O_8$ mediated metal free oxidative coupling of alcohols with 1, 2-diaminobenzenes for synthesis of benzimidazoles, photophysical and DFT studies. J Mol Struct. 2023;1294:136431. https://doi.org/10.1016/j.molstruc.2023.136431.
4. Roque JP, Rosado MT, Fausto R, Reva I. Dual photochemistry of benzimidazole. J Org Chem. 2023;88(5):2884–97. https://doi.org/10.1021/acs.joc.2c02560.
5. Refaat HM. Synthesis and anticancer activity of some novel 2-substituted benzimidazole derivatives. Eur J Med Chem. 2010;45(7):2949–56. https://doi.org/10.1016/j.ejmech.2010.03.022.
6. Kumar K, Awasthi D, Lee SY, Zanardi I, Ruzsicska B, Knudson S, Tonge PJ, Slayden RA, Ojima I. Novel trisubstituted benzimidazoles, targeting Mtb FtsZ, as a new class of antitubercular agents. J Med Chem. 2011;54(1):374–81. https://doi.org/10.1021/jm1012006.
7. Starčević K, Kralj M, Ester K, Sabol I, Grce M, Pavelić K, Karminski-Zamola G. Synthesis, antiviral and antitumor activity of 2-substituted-5-amidino-benzimidazoles. Bioorg Med Chem. 2007;15(13):4419–26. https://doi.org/10.1016/j.bmc.2007.04.032.
8. Gaba M, Singh S, Mohan C. Benzimidazole: an emerging scaffold for analgesic and anti-inflammatory agents. Eur J Med Chem. 2014;76:494–505. https://doi.org/10.1016/j.ejmech.2014.01.030.
9. Law C, Yeong KY. Benzimidazoles in drug discovery: a patent review. ChemMedChem. 2021;16(12):1861–77. https://doi.org/10.1002/cmdc.202100004.
10. Khodja IA, Boulebd H, Bensouici C, Belfaitah A. Design, synthesis, biological evaluation, molecular docking, DFT calculations and in silico ADME analysis of (benz) imidazole-hydrazone derivatives as promising antioxidant, antifungal, and anti-acetylcholinesterase agents. J Mol Struct. 2020;1218:128527. https://doi.org/10.1016/j.molstruc.2020.128527.
11. Patel M, Avashthi G, Gacem A, Alqahtani MS, Park HK, Jeon BH. A Review of Approaches to the Metallic and Non-Metallic Synthesis of Benzimidazole (BnZ) and Their Derivatives for Biological Efficacy. Molecules. 2023;28(14):5490. https://doi.org/10.3390/molecules28145490.
12. Al-Wasidi AS, Refat MS, Naglah AM, Elhenawy AA. Different potential biological activities of benzimidazole derivatives. Egypt J Chem. 2021;64(5):2631–46. https://doi.org/10.21608/ejchem.2021.71477.3570.
13. Işık A, Çevik UA, Çelik I, Bostancı HE, Karayel A, Gündoğdu G, Ince U, Koçak A, Özbay Y, Kaplancıklı ZA. Benzimidazole-hydrazone derivatives: Synthesis, in vitro anticancer, antimicrobial, antioxidant activities, in silico DFT and ADMET studies. J Mol Struct. 2022;1270:133946. https://doi.org/10.1016/j.molstruc.2022.133946.
14. Caleta I, Kralj M, Marjanovic M, Bertosa B, Tomic S, Pavilovic G, Pavelic K, Karminski-Zamola G. Novel cyano- and amidinobenzothiazole derivatives: synthesis, antitumor evaluation, and X-ray and quantitative structure – activity relationship (QSAR). Anal J Med Chem. 2009;52:1744–56. https://doi.org/10.1021/jm801566q.
15. Parkin DM. Global cancer statistics in the year 2000. Lancet Oncol. 2001;2(01):596. https://doi.org/10.1016/S1470-2045(01)00486-7.
16. Baykara O. Current modalities in treatment of cancer. Balikesir Health Sci J. 2016;5(3):154–65.
17. Neidle S. Cancer Drug Design and Discovery. 2nd ed. London: Elsevier Inc; 2013.
18. Yangın S, Tanman Ü, Cansaran-Duman D. Pharmaceutical applications based on next generation sequencing technology in oncologic drug development. Turk Hij Den Biyol Derg. 2019;76(4):473–86.
19. Choi HJ, Jeong YJ, Kim J, Hoe HS. EGFR is a potential dual molecular target for cancer and Alzheimer's disease. Front Pharmacol. 2023;14:1238639. https://doi.org/10.3389/fphar.2023.1238639.
20. Liang L, Lin R, Xie Y, Lin H, Shao F, Rui W, Chen H. The role of cyclophilins in inflammatory bowel disease and colorectal cancer. Int J Biol Sci. 2021;17(10):2548–60. https://doi.org/10.7150/ijbs.58671.
21. Chuang HH, Zhen YY, Tsai YC, Chuang CH, Hsiao M, Huang MS, Yang CJ. FAK in cancer: from mechanisms to therapeutic strategies. Int J Mol Sci. 2022;23(3):1726. https://doi.org/10.3390/ijms23031726.
22. El-Gowily AH, Loutfy SA, Ali EM, Mohamed TM, Mansour MA. Tioconazole and chloroquine act synergistically to combat doxorubicin-induced toxicity via inactivation of PI3K/AKT/mTOR signaling mediated ROS-dependent apoptosis and autophagic flux inhibition in MCF-7 breast cancer cells. Pharmaceuticals. 2021;14(3):254. https://doi.org/10.3390/ph14030254.
23. Sharma J, Bhardwaj VK, Das P, Purohit R. Identification of naturally originated molecules as γ-aminobutyric acid receptor antagonist. J Biomol Struct Dyn. 2021;39(3):911–22. https://doi.org/10.1080/07391102.2020.1720818.
24. George Priya Doss C, Rajasekaran R, Sudandiradoss C, Ramanathan K, Purohit R, Sethumadhavan R. A novel computational and structural analysis of nsSNPs in CFTR gene. Genome Med. 2008;2:23–32. https://doi.org/10.1007/s11568-008-9019-8.
25. Kumar A, Rajendran V, Sethumadhavan R, Purohit R. Evidence of colorectal cancer-associated mutation in MCAK: a computational report. Cell Biochem Biophys. 2013;67:837–51. https://doi.org/10.1007/s12013-013-9572-1.
26. Salomon-Ferrer R, Case DA, Walker RC. An overview of the Amber biomolecular simulation package. Wiley Interdiscip Rev : Comput Mol Sci. 2013;3(2):198–210. https://doi.org/10.1002/wcms.1121.
27. Liu H, Jin Y, Ding H. (2023). MDBuilder: a PyMOL plugin for the preparation of molecular dynamics simulations. Brief Bioinform. 2023;24(2):bbad057. https://doi.org/10.1093/bib/bbad057.
28. Kumar A, Rajendran V, Sethumadhavan R, Purohit R. Molecular dynamic simulation reveals damaging impact of RAC1 F28L mutation in the switch I region. PLoS ONE. 2013;8(10):e77453. https://doi.org/10.1371/journal.pone.0077453.
29. Bouchekioua S, Akkoc S, Menacer R. In vitro and in silico studies on benzimidazole-based compounds. ChemistrySelect. 2024;9(1):e202304347. https://doi.org/10.1002/slct.202304347.
30. Başat Dereli D, Akkoc S, Çubuk Demiralay E. Protonation constant determination of some benzimidazole-based drug candidates by reverse phase liquid chromatography method and cytotoxic activity studies. ChemistrySelect. 2023;8(28):e202301192. https://doi.org/10.1002/slct.202301192.

31. Yavuz SÇ, Akkoç S, Tüzün B, Şahin O, Saripinar E. Efficient synthesis and molecular docking studies of new pyrimidine-chromeno hybrid derivatives as potential antiproliferative agents. Synth Commun. 2021;51(14):2135–59. https://doi.org/10.1080/00397911.2021.1922920.
32. Al-Janabi IAS, Yavuz SÇ, Köprü S, Tapera M, Kekeçmuhammed H, Akkoç S, Tüzün B, Patat Ş, Sarıpınar. E. (2022). Antiproliferative activity and molecular docking studies of new 4-oxothiazolidin-5-ylidene acetate derivatives containing guanylhydrazone moiety. J Mol Struct. 2022;1258:132627. https://doi.org/10.1016/j.molstruc.2022.132627.
33. Yavuz SÇ, Akkoç S, Türkmenoğlu B, Sarıpınar E. Synthesis of novel heterocyclic compounds containing pyrimidine nucleus using the Biginelli reaction: Antiproliferative activity and docking studies. J Heterocycl Chem. 2020;57(6):2615–27. https://doi.org/10.1002/jhet.3978.
34. Yavuz SÇ, Akkoç S, Sarıpınar E. The cytotoxic activities of imidazole derivatives prepared from various guanylhydrazone and phenylglyoxal monohydrate. Synth Commun. 2019;49(22):3198–209. https://doi.org/10.1080/00397911.2019.1661481.
35. Spartan'10. version 1.1.0. Wavefunction, Inc. Irvine, CA. 2010.
36. Wałęsa R, Kupka T, Broda MA. Density functional theory (DFT) prediction of structural and spectroscopic parameters of cytosine using harmonic and anharmonic approximations. Struct Chem. 2015;26:1083–93. https://doi.org/10.1007/s11224-015-0573-0.
37. Butt SS, Badshah Y, Shabbir M, Rafiq M. Molecular docking using chimera and autodock vina software for nonbioinformaticians. JMIR Bioinfor Biotech. 2020;1(1):e14232. https://doi.org/10.2196/14232.
38. Veiga-Matos J, Morales AI, Prieto M, Remião F, Silva R. Study models of drug–drug interactions involving p-glycoprotein: the potential benefit of p-glycoprotein modulation at the kidney and intestinal levels. Molecules. 2023;28(22):7532. https://doi.org/10.3390/molecules28227532.
39. Desale VJ, Mali SN, Thorat BR, Yamgar RS, Synthesis. admetSAR predictions, DPPH radical scavenging activity, and potent anti-mycobacterial studies of hydrazones of substituted 4-(anilino methyl) benzohydrazides (Part 2). Curr Comput -Aided Drug Des. 2021;17(4):493–503. https://doi.org/10.2174/1573409916666200615141047.
40. Al Azzam KM, Negim ES, Aboul-Enein HY. ADME studies of TUG-770 (a GPR-40 inhibitor agonist) for the treatment of type 2 diabetes using SwissADME predictor: In silico study. J Appl Pharm Sci. 2022;12(4):159–69. https://doi.org/10.7324/JAPS.2022.120418.
41. Sharma S, Sharma A, Gupta U. Molecular docking studies on the anti-fungal activity of allium sativum (garlic) against mucormycosis (black fungus) by BIOVIA discovery studio visualizer 21.1. 0.0. 2021. https://doi.org/10.21203/rs.3.rs-888192/v1.
42. Muhammed MT, Kokbudak Z, Akkoc S. Cytotoxic activities of the pyrimidine-based acetamide and isophthalimide derivatives: an in vitro and in silico studies. Mol Simul. 2023;49(10):982–92. https://doi.org/10.1080/08927022.2023.2202766.
43. Muhammed MT, Mustafa ER, Akkoc S. Molecular modeling and in vitro antiproliferative activity studies of some imidazole and isoxazole derivatives. J Mol Struct. 2023;1282:135066. https://doi.org/10.1016/j.molstruc.2023.135066.
44. Yavuz SÇ. Molecular docking and reactive sites identification (Homo–Lumo, Mep) of allicin and diallyl disulfide: potential anticancer inhibitor. Black Sea J Sci. 2023;13(4):1523–39. https://doi.org/10.31466/kfbd.1307190.
45. Bahgat K, Fraihat S. Normal coordinate analysis, molecular structure, vibrational, electronic spectra and NMR investigation of 4-Amino-3-phenyl-1H-1,2,4-triazole-5(4H)- thione by ab initio HF and DFT method. Spectrochim Acta Mol Biomol Spectrosc. 2015;135:1145–55. https://doi.org/10.1016/j.saa.2014.05.081.
46. Lakshminarayanan S, Jeyasingh V, Murugesan K, Selvapalam N, Dass G. Molecular electrostatic potential (MEP) surface analysis of chemo sensors: An extra supporting hand for strength, selectivity & non-traditional interactions. J Photochem Photobiol. 2021;6:100022. https://doi.org/10.1016/j.jpap.2021.100022.
47. Celik S, Demircioğlu Z, Yurdakul S, Büyükgüngör O. Synthesis, crystal structure, Hirshfeld surface analysis and molecular docking analysis of new cadmium (II) iodide complex with the pyridine, 4-(1,1-dimethylethyl). J Coord Chem. 2022;75(1–2):84–106. https://doi.org/10.1080/00958972.2022.2031168.
48. Lee YT, Tan YJ, Oon CE. Benzimidazole and its derivatives as cancer therapeutics: The potential role from traditional to precision medicine. Acta Pharm Sin B. 2023;13(2):478–97. https://doi.org/10.1016/j.apsb.2022.09.010.
49. Satija G, Sharma B, Madan A, Iqubal A, Shaquiquzzaman M, Akhter M, Parvez S, Khan MA, Alam MM. Benzimidazole based derivatives as anticancer agents: Structure activity relationship analysis for various targets. J Heterocycl Chem. 2022;59(1):22–66. https://doi.org/10.1002/jhet.4355.
50. Huynh TKC, Nguyen THA, Tran NHS, Nguyen TD, Hoang TKD. A facile and efficient synthesis of benzimidazole as potential anticancer agents. J Chem Sci. 2020;132:1–9. https://doi.org/10.1007/s12039-020-01783-4.
51. Çalışkan ŞG, Genç O, Erol F, Sarıkavaklı N. Molecular docking, Homo-Lumo, quantum chemical computation and bioactivity analysis of vic-dioxim derivatives bearing hydrazone group ligand and their NiII and CuII complexes. Gazi Univ J Sci Part A: Eng Innov. 2022;9(3):299–313. https://doi.org/10.54287/gujsa.1160449.
52. Shaker B, Ahmad S, Lee J, Jung C, Na D. In silico methods and tools for drug discovery. Comput Biol Med. 2021. https://doi.org/10.1016/j.compbiomed.2021.104851. 137,104851.
53. Prieto-Martínez FD, López-López E, Juárez-Mercado KE, Medina-Franco JL. (2019). Computational drug design methods-current and future perspectives. In Silico Drug Des. 2019;19–44. https://doi.org/10.1016/B978-0-12-816125-8.00002-X.
54. Dashti Y, Grkovic T, Quinn RJ. Predicting natural product value, an exploration of anti-TB drug space. Nat Prod Rep. 2014;31(8):990–8. https://doi.org/10.1039/C4NP00021H.
55. Nazreen S. Design, synthesis and molecular docking studies of thiazolidinediones as PPAR-agonists and thymidylate synthase inhibitors. Arch Pharm. 2021;354:2100021. https://doi.org/10.1002/ardp.202100021.
56. Lipinski CA, Hicks SD, Callaway CW. Normoxic ventilation during resuscitation and outcome from asphyxial cardiac arrest in rats. Resuscitation. 1999;42(3):221–9. https://doi.org/10.1016/S0300-9572(99)00083-0.
57. Lipinski CA, Lombardo F, Dominy BW, Feeney PJ. Experimental and computational approaches to estimate solubility and permeability in drug discovery and development settings. Adv Drug Deliv Rev. 2001;4:3–26. https://doi.org/10.1016/s0169-409x(00)00129-0.
58. Banerjee P, Ulker OC. Combinative ex vivo studies and in silico models ProTox-II for investigating the toxicity of chemicals used mainly in cosmetic products. Toxicol Mech Methods. 2022;32(7):542–8. https://doi.org/10.1080/15376516.2022.2053623.

Publisher's Note